

Transport and magnetic properties of metallic $\text{La}_{1-x}\text{Pb}_x\text{NiO}_3$ ($0.0 < x < 0.1$)

Sudipta Pal, B. K. Chaudhuri, S. Neeleshwar, Y. Y. Chen, and H. D. Yang

Citation: *Journal of Applied Physics* **97**, 043707 (2005); doi: 10.1063/1.1852691

View online: <http://dx.doi.org/10.1063/1.1852691>

View Table of Contents: <http://scitation.aip.org/content/aip/journal/jap/97/4?ver=pdfcov>

Published by the [AIP Publishing](#)



Re-register for Table of Content Alerts

Create a profile.



Sign up today!



Transport and magnetic properties of metallic $\text{La}_{1-x}\text{Pb}_x\text{NiO}_{3-\delta}$ ($0.0 \leq x \leq 0.1$)

Sudipta Pal and B. K. Chaudhuri^{a)}

Department of Solid State Physics, Indian Association for The Cultivation of Science, Kolkata-700032, India

S. Neeleshwar and Y. Y. Chen

Institute of Physics, Academia Sinica, Taipei, Taiwan, Republic of China

H. D. Yang

Department of Physics, National Sun Yat Sen University, Kaohsiung-804, Taiwan, Republic of China

(Received 1 July 2004; accepted 1 December 2004; published online 25 January 2005)

Transport properties (resistivity and thermoelectric power) of Pb doped LaNiO_3 viz. $\text{La}_{1-x}\text{Pb}_x\text{NiO}_{3-\delta}$ ($0.0 \leq x \leq 0.1$) show metallic behavior over a wide range of temperature (10–550 K). Pb doping (up to 10%) at the La site does not destroy the metallic behavior of LaNiO_3 . The paramagnetic susceptibility χ decreases with Pb doping. Above 50 K, χ is almost temperature independent and exhibits Pauli like features with a small additional Curie law contribution. The resistivity ρ increases with Pb doping though the thermoelectric power does not change proportionately, indicating that Pb doping does not introduce much disorder in the system. A linear T dependence of ρ observed above 150 K suggests the importance of electron–phonon (el–ph) interactions but at temperature below 150 K, ρ follows a $T^{1.5}$ dependence. The estimated el–ph interaction constant λ increases (0.80–2.53) with Pb doping ($x=0.0$ –0.1). No saturation of resistivity has been observed even up to 550 K with $x \leq 0.1$. The phonon frequency $\nu_{\text{ph}} \sim 3444 \text{ cm}^{-1}$ of the undoped sample calculated from the absorption peak of the Fourier transform infrared spectra agrees well with that at $\sim 3025 \text{ cm}^{-1}$ estimated from the reported heat capacity data. © 2005 American Institute of Physics. [DOI: 10.1063/1.1852691]

I. INTRODUCTION

Among the transitional–metal–oxides, rare-earth nickelates are very well known for their interesting and unusual metallic conductivity down to liquid helium temperature. The perovskite oxide LaNiO_3 is different from the other rare-earth nickelates^{1–3} due to its metallic behavior over a wide range of temperature. This highly conducting compound is also an interesting material because of its potential applications as metallic interconnects (or electrodes) in thin-film oxide electronics and the possibility of its use as a catalyst for oxygen electrodes in aqueous alkaline solution batteries. Earlier studies^{1–3} showed that this compound is rhombohedrically distorted and a narrow band metallic conductor with nominally Ni^{3+} ions in a near-octahedral coordination. It has been further shown that LaNiO_3 is metallic with a large Pauli-type magnetic susceptibility, which has been interpreted in terms of a Stoner enhancement³ based on ferromagnetic correlation of electrons in the quarter filled e_g band associated with Ni^{3+} ions in the $3d^7$ configuration. Detailed susceptibility measurement has revealed a weak T dependence of χ at intermediate temperature and Curie–Weiss behavior above 50 K. This magnetic property might be responsible for locking the superconducting transition in this system.

Previous literature survey^{1–5} shows that our understanding of the metallic behavior of nickelates is still in a rudimentary state. It has been reported that the low temperature

(<10 K) resistivity data follows a $T^{0.5}$ dependence.⁴ A T^2 dependence (corresponding to electron–electron interaction) of resistivity in this compound⁵ at lower temperature has also been reported. On the contrary, a $T^{1.5}$ dependence has been observed at higher temperatures⁵ (150–300 K). Above room temperature (i.e. $T > 300$ K), the resistivity behavior is not well described. The metal insulator transition in the rare-earth nickelates RNiO_3 is a charge-transfer type. The charge-transfer band gap lies between the occupied oxygen $2p$ valence state and the unoccupied Ni $3d$ conduction band. It is shown that the band gap of RNiO_3 lies near the insulator–metal boundary where charge-transfer gaps are small.⁶ However, in the case of LaNiO_3 , the charge-transfer gap becomes zero as the valence band and conduction band overlap. Elaborate study of the LaNiO_3 system doped with other divalent ions (viz. Pb) is needed for a deeper understanding of the transport and other basic properties associated with the electronic interaction in these nickelates.

In LaNiO_3 , divalent cation doping may compensate charge in the following ways:

- $\text{La}_{1-x}^{3+}\text{M}_x^{2-}\text{Ni}_{1-x}^{3+}\text{Ni}_x^{4+}\text{O}_3$
- $\text{La}_{1-x}^{3+}\text{M}_x^{2-}\text{Ni}^{3+}\text{O}_{3-x/2}$
- $\text{La}_{1-x}^{3+}\text{M}_x^{2-}\text{Ni}_{1-x}^{3+}\text{Ni}_x^{2+}\text{O}_{3-x}$

Considering the similar charge compensation in LaNiO_3 , it is reasonable to expect that the latter two coexist. Doping of divalent cations may change oxygen stoichiometry as discussed above and affect transport and magnetic properties. In the present article we have reported the affect of partial replacement of La with a divalent ion (viz. Pb) from the study

^{a)}Author to whom correspondence should be addressed; electronic mail: sspbkc@mahendra.iacs.res.in

of transport and magnetic properties of the single phase $\text{La}_{1-x}\text{Pb}_x\text{NiO}_{3-\delta}$ ($0.0 \leq x \leq 0.1$ and $\delta < 0.1$) system showing metallic behavior over a wide range of temperature (10–550 K). We have also analyzed the experimental data to elucidate the interactions present in the metallic oxide.

II. EXPERIMENT

The samples $\text{La}_{1-x}\text{Pb}_x\text{NiO}_{3-\delta}$ ($0.0 \leq x \leq 0.3$) were prepared by the liquid mix technique. First, stoichiometric amounts of La_2NO_3 , PbNO_3 , and NiNO_3 were dissolved in water. The water was removed by a gentle dehydration process giving a green solid, which decomposed into a fine black powder at 450 °C heated in air. The resultant powder was heated to 900 °C with intermediate grinding to obtain a single-phase perovskite.

All the prepared samples were characterized by x-ray diffraction with a $\text{Cu } K_\alpha$ radiation wavelength of $\lambda = 1.541 \text{ \AA}$. The Rietveld analysis of the diffraction data was performed using the DBWS program. Temperature dependent ρ was measured with a standard four probe technique from 10 to 550 K. Thermoelectric power was measured using a standard technique in the range 80–300 K. All the experimental data were collected in the heating direction. The temperature measurements were made with an accuracy of $\pm 0.2 \text{ K}$ or better. The dc magnetic susceptibility measurement was made using a Quantum Design superconducting quantum interference device magnetometer under field cooled (FC) and zero field cooled (ZFC) conditions at an external magnetic field 1 kOe. The room temperature Fourier transform infrared (FTIR) spectra were taken by a Perkin Elmer (model 783) infrared spectrometer.

III. RESULTS AND DISCUSSION

X-ray powder diffraction patterns of two samples with $x=0.3$ and 0.05 are shown in Fig. 1. Secondary phases of NiO were observed when $x > 0.1$. For a single-phase sample, only a certain concentration of Pb ($x \leq 0.1$) can be doped at the La site in LaNiO_3 . In a hexagonal unit cell, the estimated lattice parameters for LaNiO_3 are $a=5.46 \text{ \AA}$, $c=13.19 \text{ \AA}$. These values agree well with those reported earlier.⁴ The small increase of lattice parameters with Pb doping is believed to be due to the larger ionic radius of Pb compared to La. The temperature dependence of magnetic susceptibility $\chi(T)$ measured at 1 kOe is shown in Fig. 2. A number of interesting features are evident from the magnetic susceptibility data. All the samples show an almost temperature independent Pauli-like magnetic susceptibility with a sharp rise below 50 K. The magnetic structure in the nickelates is quite different from that of the manganites. In the rare earth manganites, the e_g orbital ordering can be explained in terms of a strong Jahn–Teller effect.⁷ Since no appreciable Jahn–Teller distortion has been observed in RNiO_3 (R =rare earth) perovskites, the existence of an orbital superlattice is invoked solely to explain the existence of such an unusual magnetic structure.⁸ The temperature dependent magnetic susceptibility $\chi(T)$ of the present Pb doped sample (above 50 K) has been observed to follow the expression

$$\chi(T) = \chi(0) - \alpha T^2 + C/T. \quad (1)$$

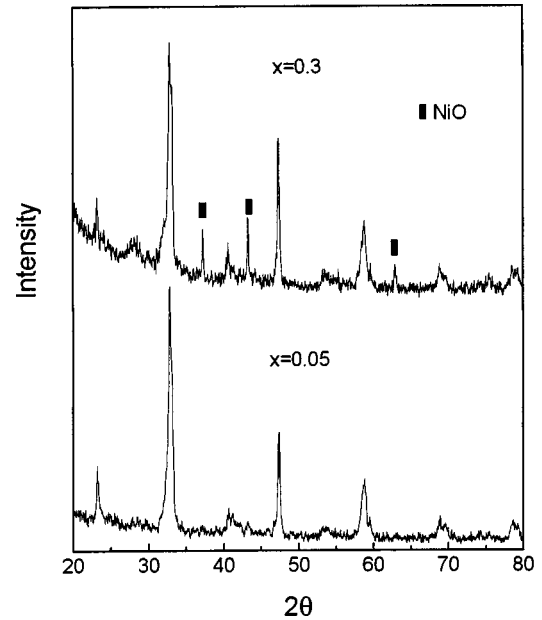


FIG. 1. X-ray powder diffraction patterns of the undoped LaNiO_3 and the doped $\text{La}_{0.7}\text{Pb}_{0.3}\text{NiO}_3$ samples. A secondary phase of NiO is observed for the sample $\text{La}_{0.7}\text{Pb}_{0.3}\text{NiO}_3$ with $x > 0.1$ (not studied in the present article).

Although the origin of the second term is unclear, it provides an empirical temperature dependence of the Pauli susceptibility.³ One observes little temperature dependence of the susceptibility even at 300 K, which accounts for a small fraction of the Pauli contribution. The third term represents a Curie law type contribution with Curie constant C . The values of the constant parameters best fitting the experimental data are given in Table I. The values of a and C decrease with the increase of Pb doping. Using the relation $\chi^{\text{Pauli}} = \mu_B^2 N(E_F)$, where μ_B is the Bohr magneton, we estimate the experimental band-structure density of electron states $N(E_F)$ at the Fermi level for both the spin directions.⁵

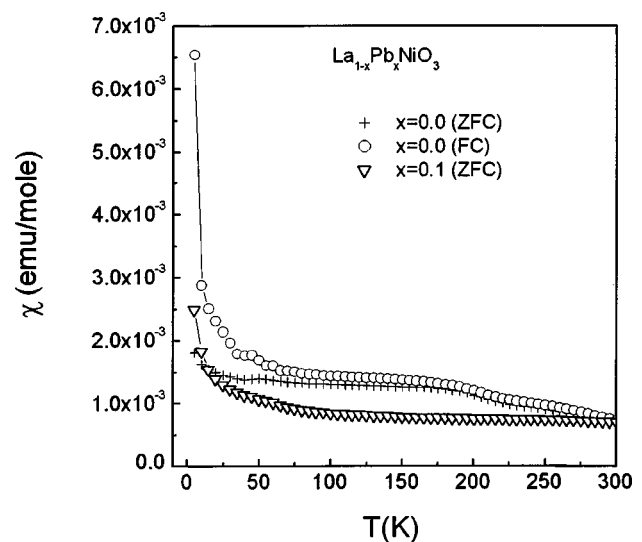


FIG. 2. Temperature dependence of the molar magnetic susceptibility χ of the Pb doped samples $\text{La}_{1-x}\text{Pb}_x\text{NiO}_{3-\delta}$ ($x=0.0$ and 0.1). At lower temperature $T < 200 \text{ K}$, a difference between ZFC and FC values is seen for the undoped LaNiO_3 sample. The value of χ decreases with the increase of Pb doping concentration x .

TABLE I. Some important parameters estimated from the dc susceptibility data using Eq. (1) for different Pb doped sample viz. $\text{La}_{1-x}\text{Pb}_x\text{NiO}_{3-\delta}$ with $x=0.0, 0.05, \text{ and } 0.1$.

	LaNiO_3		$\text{La}_{0.95}\text{Pb}_{0.05}\text{NiO}_{3-\delta}$		$\text{La}_{0.9}\text{Pb}_{0.1}\text{NiO}_{3-\delta}$	
	FC	ZFC	FC	ZFC	FC	ZFC
$\chi(0)$ (emu/mol)	14.4×10^{-4}	13.7×10^{-4}	9.6×10^{-4}	8.9×10^{-4}	6.6×10^{-4}	6.6×10^{-4}
a (emu/ K^2 mol)	8.77×10^{-9}	7.11×10^{-9}	3.33×10^{-9}	3.21×10^{-9}	1.80×10^{-10}	1.50×10^{-10}
C (emu K/mol)	1.69×10^{-3}	1.92×10^{-3}	4.00×10^{-3}	4.90×10^{-3}	18×10^{-3}	16×10^{-3}
$N(E_F)$ ($\text{eV}^{-1} \text{cm}^{-3}$)	...	4.37×10^{23}	...	2.89×10^{23}	...	2.12×10^{23}

The estimated values of $N(E_F)$ given in Table I agree quite well with those reported earlier,⁵ suggesting strong electron correlation in these materials. The values of $N(E_F)$ decreases (decreasing conductivity) with the increase of Pb doping. It has already been shown¹⁰ that the metallic behavior of LaNiO_3 is due to the overlapping of the oxygen O^{2-} and the Ni^{3+} bands. Decreasing conductivity with increasing Pb concentration reduces this overlapping character (in Fig. 3). In other words, a decrease in $N(E_F)$ is associated with an increased electron localization, which is actually observed in the oxygen deficient LaNiO_{3-x} system¹⁰ showing metal to semiconductor transition. The existence of very few Ni^{2+} ions cannot be completely ruled out. However, considering the charge compensation calculation discussed earlier, it can be said that the concentration of Ni^{2+} ions is insignificantly lower than that of Ni^{3+} .

Figures 4 and 5 show the temperature dependent electrical resistivity ρ of $\text{La}_{1-x}\text{Pb}_x\text{NiO}_{3-\delta}$ ($0.0 \leq x \leq 0.1$). Although the higher Pb doped ($x > 0.1$) samples show metallic character up to 300 K with higher resistivity, they have not been studied since these samples did not show pure single-phase behavior. The present Pb doped ($x < 0.1$) oxides have a posi-

tive temperature coefficient of resistivity down to the lowest temperature (10 K) studied, a typical metallic character. The room temperature (300 K) resistivity of LaNiO_3 is $\sim 1.6 \text{ m}\Omega \text{ cm}$, which is similar to reported results.³ The increase of resistivity with increasing Pb content should be due to changes in the valence state and oxygen coordination of Ni ions in the lattice. It is known that for the RNiO_3 system, resistivity decreases with increasing ionic radius R . Due to the larger ionic radius of Pb compared to La, the average ionic radius of R increases with Pb doping at the La site in LaNiO_3 . It is therefore expected that the resistivity should decrease with Pb doping. However, we observed an increase of resistivity with Pb doping. This behavior can be explained by considering the change of band structure due to change in oxygen coordination of Ni^{3+} ions as a result of Pb doping.¹⁰ The change of resistivity due to grain boundary contribution is considered to be negligible since the grain size of the doped sample remains almost the same with small Pb doping ($x < 0.1$). The temperature dependent resistivity behavior of the samples can be distinctly separated into two regions over the temperature region 10–550 K. At temperature lower than 150 K resistivity data follow the equation

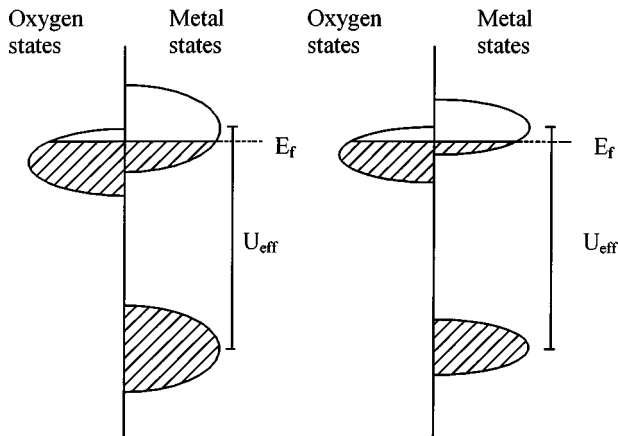


FIG. 3. Proposed band scheme to explain the conductivity behavior of $\text{La}_{1-x}\text{Pb}_x\text{NiO}_{3-\delta}$ ($x=0.0, 0.05, \text{ and } 0.1$). The left side shows the LaNiO_3 case where the overlapped Ni^{3+} and O^{2-} bands result in metallic behavior. The shadow region shows the occupied states. On the right side, the Pb doped LaNiO_3 diagram indicates higher resistivity than the corresponding undoped sample. Increasing Pb concentration leads to the narrowing of bands due to localization. The overlapping region decreases with the narrowing of the O band and thus reduces the number of occupied states.

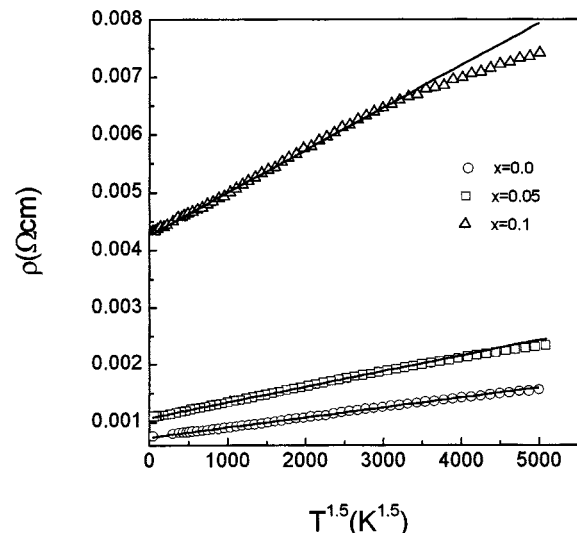


FIG. 4. Variation of resistivity as a function of $T^{-1.5}$ for the Pb doped samples $\text{La}_{1-x}\text{Pb}_x\text{NiO}_{3-\delta}$ ($x=0.0, 0.05, \text{ and } 0.1$) between 10 and 300 K. The solid lines are the best fit to the data using Eq. (2).

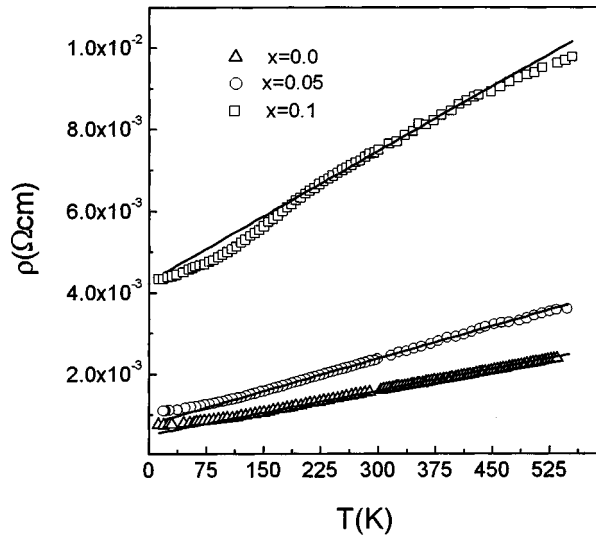


FIG. 5. Thermal variation of resistivity for the Pb doped samples $\text{La}_{1-x}\text{Pb}_x\text{NiO}_{3-\delta}$ ($x=0.0, 0.05,$ and 0.1). Solid lines are the best linear fit, indicating the dominance of el-ph interaction in these samples at higher temperature.

$$\rho(T) = \rho_0 + \rho_{1.5}T^{1.5}, \quad (2)$$

where ρ_0 and $\rho_{1.5}$ are two coefficients. The origin of $T^{1.5}$ dependence is yet to be properly clarified. It appears that both electron-electron and electron-phonon scattering contribute to the resistivity data of the system. On the other hand, at the higher temperature range 150–550 K, the metallic behavior of the resistivity data of the Pb doped $\text{La}_{1-x}\text{Pb}_x\text{NiO}_{3-\delta}$ ($0.0 \leq x \leq 0.1$) system fit well by the following equation:

$$\rho(T) = \rho_\alpha + \rho_1 T, \quad (3)$$

where ρ_α and ρ_1 are two coefficients given in Table II. This linear variation of resistivity of LaNiO_3 up to 300 K has also been observed earlier⁴ and in the present case this linearity persists well above 300 K. At higher temperature ($T > 150$ K), the observed T dependent (Fig. 5) behavior of resistivity usually arises from the el-ph scattering. With the increase of resistivity, i.e., with the increase of Pb doping, the range of the validity of the $T^{1.5}$ dependence decreases and a linear T dependence behavior dominates. We observed, as shown in Fig. 5, a linear T dependence of resistivity even up to 550 K, the maximum temperature range of our measurement. Such a linear T dependent behavior can be understood only in terms of weakly coupled el-ph interaction in the present system. The el-ph interaction constant λ is estimated

TABLE II. Different model parameters from Eqs. (2)–(4) estimated from fitting the transport data (resistivity and thermoelectric power) for $\text{La}_{1-x}\text{Pb}_x\text{NiO}_{3-\delta}$ with $x=0.0, 0.05,$ and 0.1 .

	LaNiO_3	$\text{La}_{0.95}\text{Pb}_{0.05}\text{NiO}_{3-\delta}$	$\text{La}_{0.9}\text{Pb}_{0.1}\text{NiO}_{3-\delta}$
ρ_0 ($\Omega \text{ cm}$)	0.73×10^{-3}	1.07×10^{-3}	4.20×10^{-3}
$\rho_{1.5}$ ($\Omega \text{ cm K}^{-1.5}$)	1.73×10^{-7}	2.70×10^{-7}	7.34×10^{-7}
ρ_α ($\Omega \text{ cm}$)	0.52×10^{-3}	0.78×10^{-3}	4.29×10^{-3}
(K^{-1})	2.24×10^{-3}	2.32×10^{-3}	1.35×10^{-3}
λ	0.80	1.24	2.53

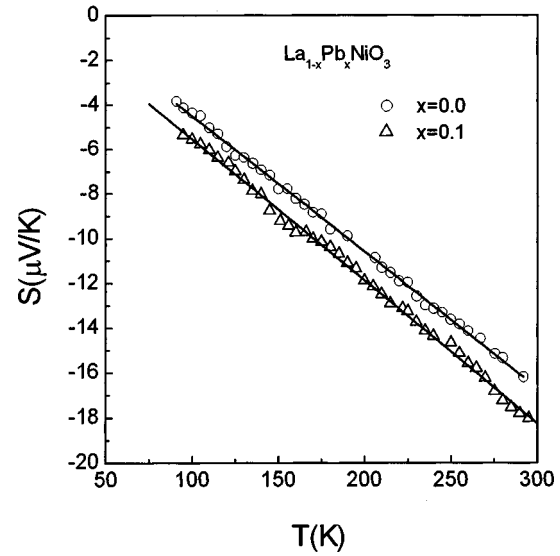


FIG. 6. Temperature dependent Seebeck coefficient S for the Pb doped samples $\text{La}_{1-x}\text{Pb}_x\text{NiO}_{3-\delta}$ ($x=0.0$ and 0.1) between 80 and 300 K. A negative thermopower suggests electron-like carriers in all the samples. Solid lines are the best fit to the data using Eq. (4).

from the slope of the resistivity versus temperature curve¹¹ using the relation

$$\lambda = \frac{\hbar \omega_p^2 [\rho(T) - \rho(0)]}{8\pi^2 k_B T}, \quad (4)$$

where ω_p is the plasma frequency and $T=300$ K. For the undoped LaNiO_3 sample, electron loss experiment¹² gives $\hbar \omega_p \approx 1$ eV from which the estimated value of λ is 0.8 [using Eq. (4)]. Since the IR spectra of the undoped and the low Pb doping samples of our investigation are almost the same, we use the undoped value of $\hbar \omega_p$ (≈ 1 eV) for all the doped samples, which give $\lambda=1.24$ and 2.53 , respectively, for the samples with $x=0.05$ and $x=0.1$ [using Eq. (4)]. The increase of the value of λ shows that el-ph interaction increases with the increase of Pb doping. In other rare earth nickelates like PrNiO_3 , high T_c superconducting oxides like La-Sr-Cu-O or Y-Ba-Cu-O , the el-ph interaction constants λ are estimated to be 0.3, 0.1, and 0.3 respectively.^{5,11} These values of λ are much smaller than those of the undoped and Pb doped LaNiO_3 system. On the other hand, in the LaMnO_3 compound, which is a semiconductor and also shows metal-insulator transition, the el-ph interaction constant¹³ is much higher (~ 9) and at high temperature a strong el-ph coupling arises due to Jahn-Teller distortion.¹⁴ We further notice that no resistivity saturation occurs in any of the three Pb doped samples up to 550 K. However, for the sample with $x=0.1$, the resistivity data show little deviation from linearity at higher temperature. This deviation from linearity is attributed to the higher value of λ in the sample. However, with higher Pb concentration, the effects of phonon anharmonicity and band-structure broadening⁹ might also disturb the linear behavior of resistivity at such a higher temperature.

Figure 6 shows the thermal variation of the Seebeck coefficient of the present Pb doped samples in the temperature range 80–300 K. All the samples show a linear and negative

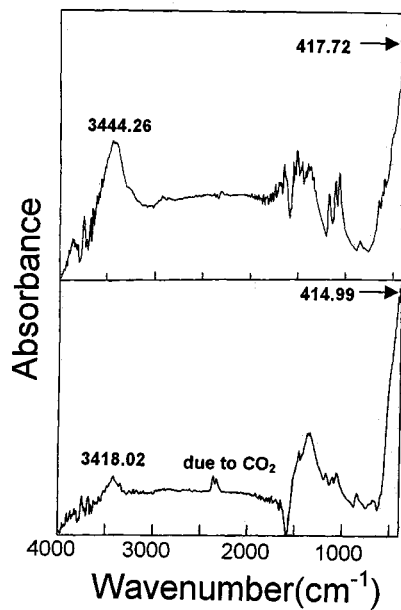


FIG. 7. FTIR spectra of the undoped LaNiO_3 (upper curve) and the Pb doped $\text{La}_{0.9}\text{Pb}_{0.1}\text{NiO}_3$ samples (lower curve). The strong absorption peak located around 417/414 cm^{-1} corresponds to the bending mode of the Ni–O–Ni bond. The peak around 3444/3418 cm^{-1} corresponds to the phonon frequency of the system.

T dependence, which is a typical metallic nature. A negative thermopower indicates the nature of the carriers may be electron-like in all the samples. A small increase in the magnitude of S indicates that Pb doping does not introduce much disorder in this system. Using the free electron model, we also estimate the energy of the Fermi level (E_F) of the system from fitting the thermopower data with the following equation:

$$S = - \frac{(\pi^2 \kappa_B^2 T)}{(3eE_F)}. \quad (5)$$

From the slope of the straight line in Fig. 6, the estimated value of E_F for LaNiO_3 is found to be 0.40 eV. The value of E_F for Pb doped samples is similar to that of the undoped sample (0.39 eV for $x=0.05$ and 0.38 eV for $x=0.1$). This suggests almost equal order of carrier density both for the Pb doped and undoped samples. The experimental density of states is 1 order higher than that estimated from band structure calculation ($\sim 10^{22}$) which suggests strong electron correlation in these materials.¹²

Finally, it is noticed from the room temperature FTIR spectroscopy, that the phonon frequency and the vibration modes in these Pb doped and undoped nickelates are also similar (Fig. 7). Interestingly, in the present Pb doped nickelates the infrared-active vibration mode is observed around 420 cm^{-1} (Fig. 7). It was reported earlier¹⁴ that in LaMnO_3 , two infrared-active vibration modes are present in the lower band at around 600 and 420 cm^{-1} . The peak around 600 cm^{-1} corresponds to the stretching mode that involves internal motion of a change in length of the Mn–O bond and the band around 420 cm^{-1} corresponds to the bending mode, which is sensitive to a change in the Mn–O–Mn bond angle. Observing the similarity, we can argue that the absorption

peak around 420 cm^{-1} is due to a change in the Ni–O–Ni bond angle. The other absorption peak due to stretching mode is not shown by the present Pb doped and undoped LaNiO_3 samples. It appears that the stretching mode is not infrared active in LaNiO_3 . Other optical studies like Raman spectroscopy etc. might explain the vibrational modes in this system. The phonon frequency ν_{ph} , estimated from the heat capacity data of Sreedhar *et al.*³ (using the relations $\beta = 234 N k_B / \theta_D^3$ and $h\nu_{\text{ph}} = k_B \theta_D$, where β is the temperature coefficient of Debye law and θ_D is the Debye temperature) is about 3025 cm^{-1} , which agrees quite well with the absorption peak of the FTIR spectra around 3444 cm^{-1} . So, the absorption peak observed in the higher frequency region ($\sim 3444 \text{ cm}^{-1}$) corresponds to the phonon frequency of the system.

IV. CONCLUSION

In summary, we have prepared and measured transport and magnetization of a new type of metallic oxide viz. $\text{La}_{1-x}\text{Pb}_x\text{NiO}_{3-\delta}$ ($0.0 < x < 0.3$) showing metallic behavior over a wide range of temperature (10–550 K). Only a very small amount of Pb ($x \leq 0.1$) can be doped to preserve the single-phase character of this perovskite. The increase in the resistivity with Pb doping can be explained by considering the change of band structure due to change in oxygen coordination of the Ni^{3+} ion. The resistivity behavior shows a $T^{1.5}$ dependence at low temperature, whereas at high temperature a linear T dependence is observed, suggesting the appreciable contribution of el–ph interaction to the resistivity. The el–ph interaction constant of these Pb doped compounds is found to be larger than those of other rare earth nickelates, high temperature superconductor material like La–Sr–Cu–O or Y–Ba–Cu–O, but smaller than those of rare earth manganites showing semiconducting–metallic transitions. There is a small Curie contribution to the susceptibility and this contribution increases with the increase of Pb concentration (keeping x within 0.1). Though Pb doping in LaNiO_3 has a large effect on the resistivity, the thermoelectric power does not change proportionately, indicating that Pb doping does not introduce much disorder in the system. Strong electron correlation is, however, observed both from resistivity and thermoelectric power data. The room-temperature FTIR spectra of the Pb doped system shows the vibration modes of these samples. The phonon frequency of the system estimated from the already reported specific heat data agrees quite well with FTIR spectra of the samples. Further investigation with the doping of other divalent ions like Sr, Ca, and alkali metals at the La site might be interesting.

ACKNOWLEDGMENT

The authors acknowledge the Department of Science and Technology, Government of India and National Science Council of Republic of China for financial support.

¹A. Wold, R. J. Arnott, and J. B. Goodenough, J. Appl. Phys. **29**, 387 (1958).

²A. K. Raychaudhuri, K. P. Rajeev, H. Srikant, and R. Mahendran, Physica B **197**, 124 (1994).

³K. Sreedhar, J. M. Honig, M. Darwin, M. McElfresh, P. M. Shand, J. Xu,

- B. C. Crooker, and J. Spalek, Phys. Rev. B **46**, 6382 (1992).
- ⁴K. P. Rajeev, G. V. Shivshankar, and A. K. Raychaudhuri, Solid State Commun. **79**, 591 (1991).
- ⁵X. Q. Xu, J. L. Peng, Z. Y. Li, H. L. Ju, and R. L. Greene, Phys. Rev. B **48**, 1112 (1993).
- ⁶J. B. Torrance, P. Lacorre, A. I. Nazzari, E. J. Ansaldo, and C. Niedermayer, Phys. Rev. B **45**, 8209 (1992).
- ⁷J. M. D. Coey, M. Viret, and S. von Molner, Adv. Phys. **48**, 167 (1999).
- ⁸M. L. Mcdarde, J. Phys.: Condens. Matter **9**, 1679 (1996).
- ⁹M. A. Paalanen, J. E. Graebner, R. N. Bhatt, and S. Sachder, Phys. Rev. Lett. **61**, 597 (1988).
- ¹⁰R. D. Sanchez, M. T. Causa, A. Caneiro, A. Butera, M. Vallet-Regi, M. J. Sayagues, J. Gonzalez-Calbet, F. Garcia-Sanz, and J. Rivas, Phys. Rev. B **54**, 16574 (1996).
- ¹¹M. Gurvitch and A. T. Fiory, Phys. Rev. Lett. **59**, 1337 (1987).
- ¹²J. Pkemp and P. A. Cox, Solid State Commun. **75**, 731 (1990).
- ¹³S. Pal, A. Banerjee, E. Rozenbarg, and B. K. Chaudhuri, J. Appl. Phys. **89**, 4955 (2001).
- ¹⁴A. J. Millis, B. I. Shraiman, and R. Mueller, Phys. Rev. Lett. **77**, 175 (1996).